Highlighting the effect of the donor on TPA-based organic, efficient sensitizers for increasing the efficiency of dye-synthesized solar cells: DFT and TD-DFT study

Mahmoud M.A. Mohammed* **& Samar T. Hassan**

Chemistry Department, Faculty of Science, New Valley University, El-Kharga 72511, Egypt.
Doi: 10.21608/nujbas.2024.345387.1028

Abstract

New derivatives of the reference dye (**ABC**) are designed with (D–π–A) architecture. A comparison between the computed geometrical parameters, optical and photovoltaic properties against those of the reference triphenylamine- (**TPA**)-based dye sensitizer **ABC** containing the cyanoacrylic acid anchor group (electron-withdrawing group), tri-phenylamine terminal electron-rich group (D) and thiophene π-spacer is introduced and investigated. The new dyes differ from **ABC** by incorporating a different group of electron-donors. The density functional theory (**DFT**) and time-dependent density functional theory (**TD-DFT**) are utilized for explaining the change in the electrochemical, absorption spectra, quantitative or qualitative descriptors, and geometry properties resulting from the incorporation of the electron donor unit. In this manuscript, the suggested computational method is applied using four functions to compare the new theoretical results vs those given experimentally for **ABC** dye. The effects made on the electronic and optical properties by incorporating moieties into donors have been discussed at length. Results of the considered dye sensitizers ensure that the E and D dyes are attractive choices for dye-synthesized solar cells (**DSSCs**) application.

Introduction

In recent years, studying solar cell properties has received much attention due to their efficiency in generating electricity and their low price compared with nuclear energy, fossil fuels, and other renewable energies [1]. Thus, searching for new strategies to reduce the cost of solar energy has become active research undertaken. One of the most important strategies is **DSSC**, which has many advantages compared with conventional solar cells such as the simplicity of manufacturing, light in weight, and environmentally friendly [2, 3]. In 1991, **DSSC** was developed by O'Regan and Grätzel [4, 5]. Several efforts have been made to improve **DSSC** performance to be another option for traditional solar cells. Heng *et al.* [6] obtained precisely the efficiency of photoelectric conversion of organic dyes for **DSSCs** based on anthracene. Valdiviezo and Palma [7] enhanced molecular rectification based on chemical and conformational changes. Yang *et al.* [8] presented a technique to predict the power conversion efficiency (P_{CE}) of **DSSCs** by developing a rational design of Dyes based on Dithienopicenocarbazole. Yang *et al.* [9] studied the 4-tert-Butyl Pyridine function theoretically and experimentally to adapt the interface energy level of **DSSCs** in its solid state.

One of the most effective charge transfers (CT) sensitizers is the ruthenium-based dye that has been applied for these cells, it improved the P_{CE} to reach up to 12% in an iodide/triiodide electrolyte solution (I^-/I_3^-)[10, 11]. Also, a lot of studies have been conducted to develop the properties and composition of these cells. As far as the authors know, the best achievement of P_{CE} reaches 13.6% which is given by the organic dye triazatruxene sensitizers [12].

The operation mechanism of a **DSSC** is well known and can be described as follows: The light falling on dyes excites electrons, which are injected into the metal oxide conduction band (CB), and for completing the circuit, a regeneration occurs in the electrolyte solution [13]. The donor-acceptor structures (D - π - A) are utilized for designing the studied organic dyes in which the photons are transferred to the acceptor from the donor (photoexcitation) and then to the semiconductor CB by anchoring group [14].

Recently, many research papers have addressed the improvement of metal-free organic allergens that can be utilized as electron sources like coumarin [15, 16, 17], carbazole [18], **TPA** [19, 20, 21], and indoline [22, 23].

One of the most important advantages of **TPA** is the ease of nitrogen center oxidation [**19**, **20**, **21**, **24**]. Indeed, **TPA** is known to bind the cationic charge on the TiO_2 surface, thus preventing reaggregation. In addition to the steric hindrance provided by **TPA**, it protects the semiconductor surface from unwanted dye accumulation [**25**]. These molecules exhibit excellent charge transport properties in electro-photo conductors due to their high drift mobility [**26**].

In the current manuscript, the **DFT** and **TD-DFT** are utilized to study characters of **TPA**-based dyes by incorporating various donors which can produce a highly stable CT to a bridge and excellent electronic properties. The suggested donors were introduced to obtain new **TPA**-based dyes with different electronic and optical properties. The tested dyes are obtained which replace X in general structure (Class A) by (**NH, O, S, GeH2**, **and SiMe2**) are shown in **Fig. 1.**

Computational details

DFT calculations are implemented by the **B3LYP** level with the 6-31G (d, p) basis sets for the geometries of the studied sensitizers. Previously established studies demonstrated that **TD-DFT** is a very accurate and efficient theory to calculate the electric properties of energy, vertical excitation, and UV spectra [**27**, **28**]. Therefore, it is known that there is a significant effect of CT excitations using different exchange and correlation (XC) functions. To choose an appropriate method, we used many XC functionals.

Table 1 summarizes the computations obtained using many **TD-DFT** functional (**B3LYP** [**29**, **30**], **CAM-B3LYP** [**31**], WB97XD [**32**], and PBE1 [**33**]) to predict the absorption spectra result of ground first excited states of **ABC** and compares it with the practical result. **Fig. 1** shows that **B3LYP** functionally agrees well with the experimental value. The **B3LYP** produced a deviation of 3 nm compared to the laboratory value. On the other hand, some previous studies have shown that **B3LYP** often produces better results [**29**, **34**]. Therefore, to predict the new sensitizers' optical properties, the **TD-B3LYP** functional is adopted with 6-311+g (d, p) basis sets, along with the conductor polarizable continuum model (CPCM) [**35**] that is combined in the Tetrahydrofuran (THF) solution. Note that the Gaussian 16 is used for getting all calculations.

Table 1: Computed excitation energies of λ_{max} (nm) with experimental absorption maxima in THF solution.

Methods	B3LYB	ωB97XD	CAM-B3LYB	PBEPBE	M062X	Exp.
λ_{max}	461	414	433	531	431	464
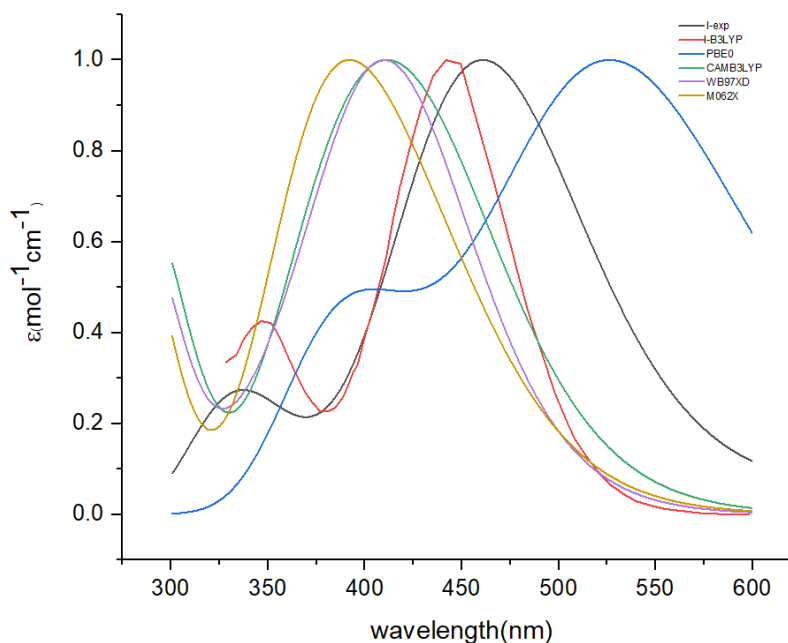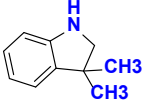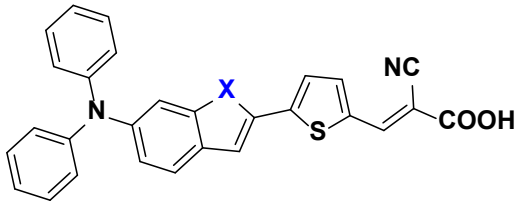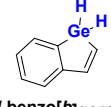
Fig. 1: Computed results of theoretical and experimental for **ABC** dye by common methods including **CAM-B3LYP**, PBE0, **B3LYP**, WB97XD, and M062X.

Results and discussion

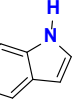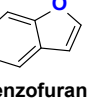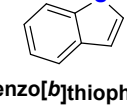It is well known that the donor is an important and effective factor in the structure of dye-sensitized solar cells, and any change in it affects the efficiency of the cell. For this reason, the incorporation of donor units into the dyes has been studied in **Fig. 1.** By presenting different moieties to the donor unit, dye molecules have been designed on Class A. Therefore, from the theoretical side, there is no problem in developing newly built structures that can be effective in the application of **DSSCs**. Tested dyes are obtained which replaced X by (NH, O, S, GeH2, and SiMe2) are shown in **Table. 2**.

On the other hand, here are some features of **TPA** that attract us to use it as a donor, some of them are the ability of light absorption of dye and reducing the aggregation on the surface of TiO_2 [36].

Table 2: Molecular structures of moieties for the tested dyes

Dyes	X of moieties	Moieties	General structure
ABC	NH-Me2	3,3-dimethylindoline	
A	GeH2	1H-benzo[b]germole	Class A
B	NH	1H-indole	
C	O	benzofuran	
D	S	benzo[b]thiophene	
E	SiH2	1H-benzo[b]silole	
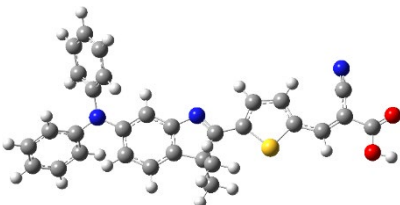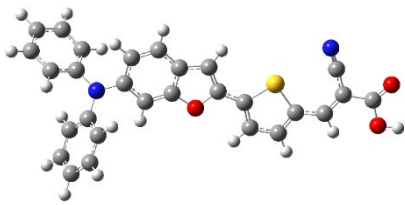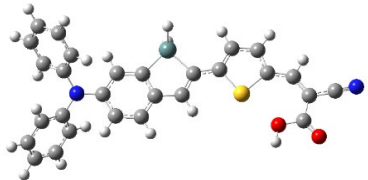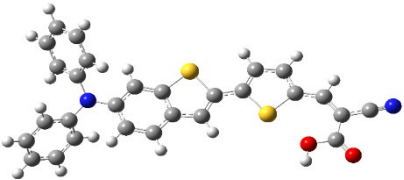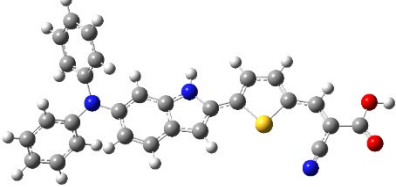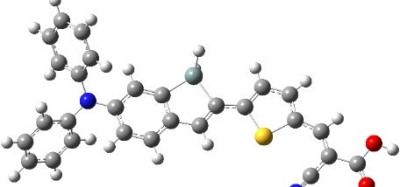
Screening of donor groups

The geometric optimization of **ABC** dye and designed derivatives are computed using **B3LYP** with the 6-31G (d,p) basis set. All dyes contain **TPA** double-ended phenyl rings twisted from the third phenyl ring level for steric hindrance [37], while the third phenyl ring is on the same plane of the molecular structure. However, the non-planarity of **TPA** in the four examined dyes could inhibit intermolecular aggregation [36]. However, a molecular coplanar structure is a preferred advantage for dyes because it decreases intramolecular recombination, which can facilitate intramolecular charge transfer (ICT) and improve molecular stability. The molecular structure of the dye also facilitates adsorption on a semiconductor surface. All dyes (**ABC, A, B, C, D, E**) show comparable co-planarity as in **Table 3**. The geometric optimization of **ABC** dye and designed derivatives are shown in **Table 4**.

Table 3: Dihedral angles of the deprotonated, anionic, cationic, and neutral forms using **B3LYP**/6-31G(d,p) theory for all dyes.

Dye	Natural form		Deprotonated form	
	ϕ_1	ϕ_2	ϕ_1	ϕ_2
ABC	0	0		
A	0	0	4	0
B	12	-1	0	0
C	0	0	0	0
D	-2	0	0	0
E	0	0	-4	0
	Cationic form		Anionic form	
	ϕ_1	ϕ_2	ϕ_1	ϕ_2
ABC	0	0	0	0
A	0	0	0	0
B	-4	0	0	0
C	0	0	0	0
D	2	0	0	0
E	0	0	0	0

Table. 4: Optimized geometric structures using **B3LYP**/6-31g (d,p) theory for all dyes

DYE	STRUCTURE	DYE	Structure
ABC		C	
A		D	
B		E	

Note: blue, red, yellow, gray, olive, and mint colors express **N**, **O**, **S**, **C, Ge,** and **Si** atoms, respectively.

Dye sensitizers electron transitions

Molecular orbitals (MOs) distribution in **A-E** dyes appear in **Table 5**, which are strongly attached to dye electronic transition properties [38]. In **DSSCs**, during the photon absorption, HOMO electrons are concentrated on **TPA**, and they will be transported to the LUMO (cyanoacrylic acid). Commonly, diagrams of HOMO and LUMO obtain the π-type MO properties. Moreover, HOMO and LUMO obtain the bonding and antibonding attraction between two neighboring segments, and consequently, the lowest energy singlet states resemble the π-π*electronic transition. The orbital properties of dyes supply them with high molar extinction coefficients. Also, it is known that LUMO electrons are injected into the semiconductor CB of TiO_2. **Table 5** shows that HOMO is mostly concentrated on **TPA** (donor) with some interaction from the π-conjugation, while the LUMO is mostly distributed to the acceptor and spacer segments. In addition, incorporation of moieties on donors affected the HOMO and LUMO energy gap

(Eg). In **Table 6,** MOs of dyes are captured by the Gauss view 6.0 version. Calculated values of the HOMO, LUMO and Eg are shown in **Table 6**, and this in turn obtains that **A**, **B,** and **C** molecules have smaller Eg than other dyes. Also, it is well known that small values of Eg make many electrons transfer faster to an excited state and are useful for longer wavelengths.

The frontier molecular orbital contribution (FMO) is a necessary aspect, it identifies the dye sensitizers CT characters [**39**]. **Fig. 2** obtains the FMO contour diagrams for calculated dye molecules. The photoexcitation properties of dye are related to the ICT from donor to acceptor units. For effective CT, LUMO of π*-orbitals of sensitizers should be located higher than the E_{CB} of TiO_2 (− 4.0 eV) surface [**30**]. Accordingly, all tested sensitizers are much higher than CB for TiO_2, which leads to an efficient injection of excited electrons. At the same time, HOMO energy levels are lower than those of redox potential I/I_3^- electrolyte (− 4.8 eV) [**40**], and the HOMO levels of tested dyes are located lower than the redox couple. Therefore, HOMO energy levels can attract electrons from the electrolyte.

Table 5: MOs main configuration of **ABC** and **A-E** dye molecules (HOMO and LUMO)

DYE	HOMO	LUMO	Density difference
ABC			
A			
B			
C			
D			
E			

The smaller Eg values for **A, B,** and **C** denote many useful features for improvement the efficiency of light harvesting (LHE) in **DSSCs**. Therefore, electron injection from the dyes is strongly permitted.

Table 6: MOs energy level (HOMO and LUMO) and Eg of dyes sensitizers implemented by **B3LYP**/6-31g (d,p) basis set

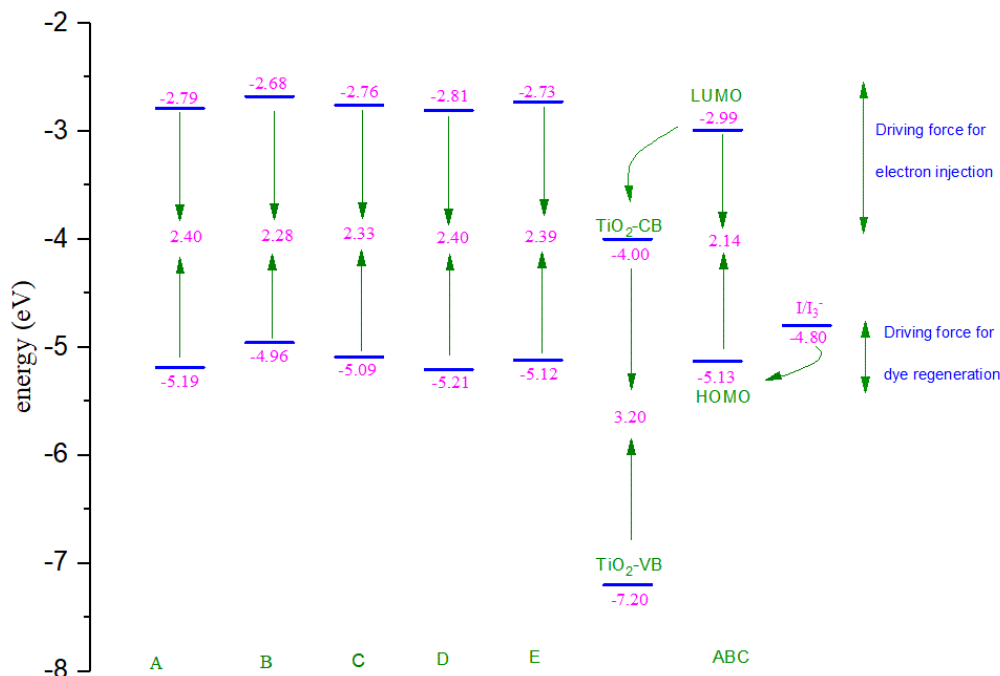|	HOMO (eV)	LUMO (eV)	Eg (eV)
ABC	-5.13	-2.99	2.14
A	-5.19	-2.79	2.40
B	-4.96	-2.68	2.28
C	-5.09	-2.76	2.33
D	-5.21	-2.81	2.40
E	-5.12	-2.73	2.39
TiO_2	-7.20	-4.00	3.20

Fig. 2: Schematic energy levels diagram of **ABC** and **A-E** dye sensitizers, TiO_2, and redox electrolyte solution(I/I_3^-).

Absorption spectra

First, the laboratory data of a maximum absorption wavelength for **ABC** molecule in THF solution is 464 nm. Second, the lowest ten excitation transitions of the computed UV-spectra in **ABC** and designed dye molecules are calculated by using the **B3LYP**/6-311+g (d,p) method as shown in **Fig. 3.** Insertion of the donor greatly affects the absorption spectra, the stimulated dyes produced bathochromic at the visible light region (550-750nm). The scientists target the visible light region to improve the performance of dye solar cells. The UV-spectra in **Fig. 3** revealed that the simulated molecules are candidates for **DSSC**. Also, **Table 7** shows the two intense peaks and their intensities at the UV spectra of examined sensitizers calculated at the **B3LYP**/6-311+g (d,p) level.

The first intense peak is the strongest one that is sharp with the longest wavelength in the region from 600to 700 nm, and it can make ICT from the donor units to the accepter. On the other hand, the second one is weak and lies in the region from 350 to 500 nm is from π→π* electronic transitions type [30, 41]. Furthermore, all investigated dyes have a longer absorption region compared to **ABC**. The maximum absorption wavelength of **A, B, C, D**, and **E** dyes lead to a red shift of 167,189,176,163, and 175 nm, respectively, compared to **ABC**. So, a red-shift of the absorption spectrum of all studied dyes leads to a better match with the solar photon flux spectrum, which has a great benefit for improving the P_{CE} of solar cells and the short-circuit current density (J_{sc})[42]. **Table 7** reveals that, for all the studied dyes, the transition of the dominant absorption bands is attached to the electron excitation from HOMO to LUMO, whereas for **ABC**, the main transition is electron transfer from HOMO-1 to LUMO. In addition, the absorption spectra diagram is presented in **Fig. 3** that shows the absorption spectra profiles of all the comparable dyes. The absorption peaks of the largest oscillator strength refer to the S0→ S1 transition for the designed dyes and the S0→S2 transition for the parent molecule **ABC**.

Table 7: Spectral characteristics of the two intense absorption wavelengths of **ABC** and its designed derivatives, calculated at the **B3LYP**/6-311+g (d,p) level

| Structures	λ_{max}^{calc}(nm)	Main configuration	Excited state	C%	f	Electronic coefficient
ABC	461	H-1→L	S_2	99.5	1.31	0.70
A	671	H→L	S_1	99.5	1.28	0.70
	442	H-1→L	S_2	98.3	0.46	0.68
	330	H→L+3	S_7	98.2	0.26	0.68
B	687	H→L	S_1	99.7	0.93	0.71
	444	H-1→L	S_2	99.4	0.48	0.70
	426	H-2→L	S_3	99.2	0.25	0.71
	374	H→L+1	S_4	96.5	0.16	0.68
	336	H-1→L+3	S_6	112.6	0.30	0.80
C	671	H→L	S_1	99.7	1.02	0.71
	436	H-1→L	S_2	99.4	0.64	0.70
	375	H→L+1	S_3	87.7	0.21	0.62
D	662	H→L	S_1	99.4	1.06	0.70
	434	H-1→L	S_2	99.4	0.61	0.70
	378	H→L+1	S_4	97.6	0.18	0.69
	328	H→L+3	S_7	97.6	0.26	0.69
E	672	H→L	S_1	99.4	1.27	0.70
	443	H-1→L	S_2	97.6	0.46	0.69
	329	H→L+3	S_7	97.6	0.26	0.69
ABC experimental	464					
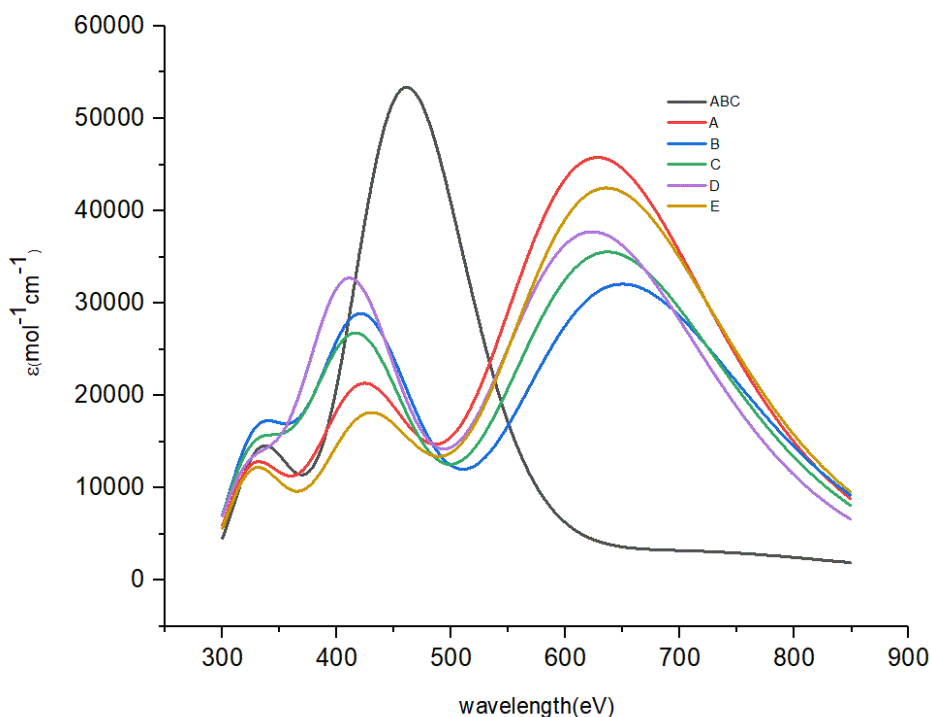
Fig. 3: Simulated absorption spectra of **ABC** and new molecules at the **TD-B3LYP**/6-311+g (d,p) level of theory in THF solution.

Overall efficiency

To estimate the **DSSCs** performance, we examined P_{CE}, J_{sc}, the short–open-circuit voltage (V_{OC}), the fill factor (FF), and the current efficiency of the incident photon (P_{inc}).

The P_{CE} is calculated by this equation [43]:

$$P_{CE} = \frac{J_{sc}\ V_{OC}\ \text{FF}}{P_{inc}}. \tag{1}$$

The V_{OC} is determined by [43]:

$$V_{OC} = E_{LUMO} - E_{CB}. \tag{2}$$

The J_{sc} of **DSSC** is expressed as [44]:

$$J_{sc} = \int_{\lambda} LHE(\lambda)\phi_{inject}\eta_{collect}d\lambda, \tag{3}$$

where ϕ_{inject} is the electron injection efficiency, $\eta_{collect}$ is the charge collection efficiency [45] and LHE is the light-harvesting efficiency

$$LHE = 1 - 10^{-f}, \tag{4}$$

where f is the oscillator strength of dye particle associated with E_{00} which is the absorption energy corresponding to (λ_{max}). Electronic injection-free energy ΔG_{inject} can be given by:

$$\Delta G_{inject} = E^{dye^*} - E_{CB}, \tag{5}$$

where E_{CB} represents the CB reduction potential (E_{CB} = −4.0 eV) of TiO_2 [46, 47], while E^{dye^*} is the dye oxidation potential energy in the excited state that is given by:

$$E^{dye^*} = E^{dye} - E_{00}, \tag{6}$$

where E^{dye} is the oxidation potential energy. Also, as shown in Eq. (3), the small total energy reorganization (λ_{total}) includes the hole and the electron energy reorganization and could improve the value of J_{sc}. And also, the small value of λ_{total} leads to a high charge transport rate [48].

Therefore, we calculate the hole and the electron reorganization energy (λ_h and λ_e) by:

$$\lambda_i = [E_0^{\pm} - E_{\pm}^{\pm}] + [E_{\pm}^0 - E_0], \tag{7}$$

where E_0 represents the energy in a stable state of the neutral molecule, $E_0^{\pm}$ expresses the energy of the anion or cation computed with the optimized structure of the neutral molecule, $E_{\pm}^{\pm}$ is the energy of the optimized cation or anion structure, and the $E_{\pm}^0$ is the cationic or anionic state energy for optimized neutral molecule.

Table 8 obtains the results of electrochemical parameters for **ABC** and other studied dyes using **B3LYP**/6-311+g(d,p). From **Table 8**, it is shown that the reorganization energy of the sensitizers **B** and **ABC** are smaller than those of other sensitizers. And it is known that, when the reorganization energy is smaller, then the recombination process is slower, and this in turn leads to a longer system life.

Since the relationship between λ_{tot} and J_{sc} is inverse [40], then the results of J_{sc} for other dyes will be better. The results in **Table 8** confirm that λ_{total} for dyes **ABC, A, B, C, D,** and **E** are 0.61, 0.62, 0.59, 1.32, 2.09, and 0.64 respectively. It is known that the efficiency of cell performance depends on the increase in the V_{OC} and J_{sc}. On the other hand, It is well-known that there is a direct relationship between V_{OC} and J_{sc}, and this matchs the results shown on **Table 8** which ensures that the increase in values of V_{OC} for the studied dyes is followed by increase in values of J_{sc} compared to those of **ABC.**

Table 8: Results of electrochemical parameters for reference and investigated dyes computed by **B3LYP**/6-311+g(d,p).

DYE	f	LHE (10^{-1})	λ_{max} (nm)	E_{oxi}^{dye}	$E_{oxi}^{dye^*}$	ΔG_{inject} (eV)	λ_e	λ_h	λ_{total}	$\Delta G_{rejection}$ (eV)	V_{OC} (eV)
ABC	1.31	0.95	461	5.13	2.44	-1.56	0.48	0.13	0.61	0.33	1.01
A	1.28	0.95	671	5.19	3.34	-0.66	0.44	0.18	0.62	0.39	1.21
	0.46	0.65	442								
	0.26	0.45	330								
B	0.93	0.88	687	4.96	3.15	-0.85	0.40	0.19	0.59	0.16	1.32
	0.48	0.67	444								
	0.25	0.44	426								
	0.16	0.31	374								
	0.30	0.50	336								
C	1.02	0.90	671	5.09	3.24	-0.76	1.48	0.16	1.32	0.29	1.24
	0.64	0.77	436								
	0.21	0.38	375								
D	1.06	0.91	662	5.21	3.33	-0.67	1.94	0.15	2.09	0.41	1.19
	0.61	0.75	434								
	0.18	0.33	378								
	0.26	0.45	328								
E	1.27	0.95	672	5.12	3.27	-0.73	0.45	0.19	0.64	0.32	1.27
	0.46	0.65	443								
	0.26	0.45	329								

Chemical reaction concepts

The chemical potential (μ), hardness (η), softness (S) and electronegativity (χ) have resulted from E_{HOMO} and E_{LUMO} for molecules as shown in **Table 9** [49]

$$\text{Chemical potential: } \mu = -(E_{LUMO} + E_{HOMO}) \ / \ 2,$$

$$\text{Chemical hardness: } \eta = (E_{LUMO} - E_{HOMO}) \ / \ 2,$$

$$\text{Chemical softness: } S = 1 \ / \ \eta = 2 \ / \ (E_{LUMO} - E_{HOMO}),$$

$$\text{Electronegativity: } \chi = -\mu = (E_{LUMO} + E_{LUMO}) \ / \ 2.$$

Table 9 shows that the TiO_2 has the lowest potential chemical value (-4.66 eV) [42] compared to that computed for **ABC, A, B, C, D, and E** dye molecules, which confirms the ease of electron transfer from donor dyes to electron acceptor semiconductor TiO_2. Also, all dyes' chemical hardness (η) is lower than that of TiO_2 (η=3.78 eV), indicating that all dyes are capable of donating electrons to the TiO_2 semiconductor. Also, we noticed that the electronegativity of TiO_2 (4.66 eV) is higher than the values of the dyes so that TiO_2 can withdraw electrons from these dyes.

Table 9: MOs energy level (HOMO and LUMO) and Eg of dyes sensitizers, μ, η, S and χ were implemented using **B3LYP**/6-31g (d,p) basis set.

	HOMO (eV)	LUMO (eV)	Eg (eV)	μ	η	S	X
ABC	-5.13	-2.99	2.14	-4.06	1.07	0.93	4.06
A	-5.16	-2.78	2.40	-3.99	1.20	0.83	3.99
B	-4.99	-2.74	2.28	-3.82	1.14	0.88	3.82
C	-5.12	-2.80	2.33	-3.93	1.17	0.86	3.93
D	-5.17	-2.80	2.40	-4.01	1.20	0.83	4.01
E	-5.16	-2.78	2.39	-3.93	1.20	0.84	3.93
TiO_2[46]	-7.20	-4.00	3.20	-5.60	1.60	0.63	5.60

Conclusion

In this research, five dyes with (D—A) structure were designed by adding fragments to the donor unit, and then the optical and chemical properties were examined and compared with laboratory dye results using the **DFT** and **B3LYP** method. The highest occupied and lowest unoccupied MOs energy levels (HOMO-LUMO), their distribution, and the E_g are studied. The V_{OC} required for electronic injection (ΔG_{inject}), total reorganization energy (λ_{total}), LHE, and absorption spectra of dyes are investigated. By comparing the results of the geometry for the new dyes with those of the reference dye, we concluded that: The best technique to match the practical outcome is that uses **B3LYP**. The reproduced dye captures higher than the reference dye in a visible light region of 600nm-750nm for the UV spectra. The V_{OC} shows better results for the dyes studied, which indicates that the rate of recombination is lower, which in turn gives the cell a longer life span. A higher V_{OC} is up to 1.32 eV in the preferred electron transfer procedure from the studied dyes to the semiconducting **TiO₂**. **TiO₂** can withdraw electrons from dyes because it has a higher electronegativity (4.66 eV) than those of all computed dyes. LHE of the investigated dyes produces results similar to the reference dye, which shows that these dyes are very promising.

References

[1] O'Regan, B., Schwartz, D.T., Large enhancement in photocurrent efficiency caused by UV illumination of the dye-sensitized heterojunction TiO_2/RuLL'NCS/CuSCN: *Initiation and potential mechanisms, Chem. Mater.,* 10 (1998) 1501-1509.

[2] Bourass, M., Benjelloun, A.T., Benzakour, M., Mcharf, M., Hamidi, M., Bouzzine, S.M., Spirau, F.S., Jarrosson, T., Lére-Porte, J.P., Sotiropoulos, J.M., The computational study of the electronic and optoelectronic properties of new materials based on thienopyrazine for application in dye solar cells, *J. Mater. Environ. Sci.*, 7 (2016) 700-712.

[3] Fitri, A., Benjelloun, A.T., Benzakour, M., Mcharf, M., Hamidi, M., Bouachrine, M., Theoretical studies of the master factors influencing the efficiency of thiazolothiazole-based organic sensitizers for DSSC, *J. Mater. Environ. Sci.*, 7 (2016) 835-844.

[4] Grätzel, M., Photoelectrochemical cells, *Nature*, 414 (2001) 338–344.

[5] Hagfeldt, A., Grätzel, M., Molecular photovoltaics, *Acc. Chem. Res.,* 33 (2000) 269–277.

[6] Heng, P., Mao, L., Guo, X., Wang, L., Zhang, J., Accurate estimation of the photoelectric conversion efficiency of a series of anthracene-based organic dyes for dye-sensitized solar cells, *J. Materials Chem.* C, 8 (2020) 2388-2399.

[7] Valdiviezo, J., Palma, J.L., Molecular rectification enhancement based on conformational and chemical modifications, *J. Phys. Chem. C,* 122 (2018) 2053-2063.

[8] Soman, S., Pradhan, S.C., Yoosuf, M., Vinayak, M.V., Lingamoorthy, S., Gopidas, K.R., Probing recombination mechanism and realization of marcus normal region behavior in DSSCs employing cobalt electrolytes and triphenylamine dyes, *J. Phys. Chem.* C, 122 (2018) 14113–14127.

[9] Yang, L., Lindblad, R., Gabrielsson, E., Boschloo, G., Rensmo, H., Sun, L., Hagfeldt, A., Edvinsson, T., Johansson, E.M.J., Experimental and theoretical investigation of the function of 4-tert-Butyl Pyridine for interface energy level adjustment in efficient solid-state dye-sensitized solar cells, *ACS Appl. Mater. Interfaces,* 10 (2018) 11572–11579.

[10] Hagfeldt, A., Boschloo, G., Sun, L., Kloo, L., Pettersson, H., Dye-Sensitized Solar Cells, *Chem. Rev.,* 110 (2010) 6595-6663.

[11] Slimi, A., Fitri, A., Benjelloun, A.T., Elkhattabi, S., Benzakour, M., Mcharf, M., Bouachrine, M., Molecular design of D-π-A-A organic dyes based on triphenylamine derivatives with various auxiliary acceptors for high-performance DSSCs, *J. Electron. Mater.*, 48 (2019) 4452–4462.

[12] Zhang, L., Yang, X.C. Wang, W.H., Gurzadyan, G.G., Li, J.J., Li, X.X., An, J.C., Yu, Z., Wang, H.X., Cai, B., Hagfeldt, A., Sun, L.C., 13.6% efficient organic dye-sensitized solar cells by minimizing energy losses of the excited state, *ACS Energy Lett.,* 4 (2019) 943–951.

[13] Kloo, L., On the early development of organic dyes for dye-sensitized solar cells, *Chem Commun.*, 49 (2013) 6580-6583.

[14] J.F., Eckert, Nicoud, J.F., Nierengarten, J.F., Liu, S.G., Echegoyen, L., Barigelletti, F., Armaroli, N., Ouali, L., Krasnikov, V.V., Hadziioannou, G., Fullerene-oligophenylenevinylene hybrids: Synthesis, electronic properties, and incorporation in photovoltaic devices, *J. Am. Chem. Soc.,* 8 (2000) 7467-7479.

[15] Han, L., Kang, R., Zu, X., Cui, Y., Gao, J., Novel coumarin sensitizers based on 2-(thiophen-2-yl)thiazole π-bridge for dye-sensitized solar cells, *Photochem. Photobiol. Sci.,* 14 (2015) 2046-2053.

[16] Liu, B., Wang, R., Mi, W., Li, X., Yu, H., Novel branched coumarin dyes for dye-sensitized solar cells: Significant improvement in photovoltaic performance by simple structure modification, *J. Mater. Chem.,* 22 (2012) 15379-15387.

[17] Wang, J., Li, M., Qi, D., Shen, W., He, R., Lin, S.H., Exploring photophysical properties of metal-free coumarin sensitizers: An efficient strategy to improve the performance of dye-sensitized solar cells, *RSC Adv.,* 4 (2014) 53927-53938.

[18] Liu, Y., He, J., Han, L., Gao, J., Influence of the auxiliary acceptor and π-bridge in carbazole dyes on photovoltaic properties*, J. Photochem. Photobiol. A*, 332 (2017) 283-292.

[19] Chen, S., Jia, H., Zheng, M., Shen, K., Zheng, H., Insight into the effects of modifying π-bridges on the performance of dye-sensitized solar cells containing triphenylamine dyes, *Phys. Chem. Chem. Phys.*, 18 (2016) 29555-29560.

[20] Prakasam, M., Anbarasan, P.M., Second-order hyperpolarizability of triphenylamine based organic sensitizers: A first principle theoretical study, *RSC. Adv.,* 6 (2016) 75242-75250.

[21] Zeng, W.D., Cao, Y.M., Bai, Y., Wang, Y.H., Shi, Y.S., Wang, P., Efficient dye-sensitized solar cells with an organic photosensitizer featuring orderly conjugated ethylene dioxythiophene and dithienosilole blocks*, Chem. Mater.*, 22 (2010) 1915–1925.

[22] Han, L., Zhao, J., Wang, B., Jiang, S., Influence of π-bridge in N-fluorenyl indoline sensitizers on the photovoltaic performance of dye-sensitized solar cells, *J. PhotoChem. Photobiol*. A, 326 (2016) 1-8.

[23] Wang, Y., Zheng, Z., Li, T., Robertson, N., Xiang, H., Wu, W., Hua, J., Zhu, W.H., Tian, H., D-A-π-A motif quinoxaline-based sensitizers with high molar extinction coefficient for quasi-solid-state dye-sensitized solar cells, *ACS Appl. Mater. Interfaces*, 8 (2016) 31016.

[24] Wang, J.W., Liu, K., Ma, L.C., Zhan, X.W., Triarylamine: A versatile platform for organic, dye-sensitized, and perovskite solar cells, *Chem. Rev.,* 116 (2016) 14675 —14725.

[25] Ning, Z., Zhang, Q., Wu, W., Pei, H., Lei, B., Tian, J.H., Starburst triarylamine based dyes for efficient dye-sensitized solar cells*, Org. Chem.,* 73 (2008) 3791–3797.

[26] Manifar, T., Rohani, S., Synthesis and analysis of triphenylamine: A review, *Canadian J. Chem. Eng.,* 82 (2004) 323-334.

[27] Mohr, T., Aroulmoji, V., Ravindran, R.S., Muller, M., Ranjitha, S., Rajarajan, G., Anbarasan, P.M., DFT and TD-DFT study on geometries, electronic structures and electronic absorption of some metal-free dye sensitizers for dye-sensitized solar cells, *Spectrochim. Acta, Part A*, 135 (2015) 1066–1073.

[28] Zhang, Y., Lai, S.L., Tong, Q.X., Lo, M.F., Ng, T.W., Chan, M.Y., Wen, Z.C., He, J., Jeff, K.S., Tang, X.L., Lee, C.S., High efficiency nondoped deep-blue organic light-emitting devices based on imidazole-π-triphenylamine derivatives, *Chem. Mater.,* 24 (2012) 61–70.

[29] Becke, A.D., Density-functional thermochemistry, III. The role of exact exchange, *J. Chem. Phys*., 98 (1993) 5648–5652.

[30] Wazzan, N.A., A DFT/TDDFT investigation on the efficiency of novel dyes with orthofluorophenyl units (A1) and incorporating benzotriazole/ benzothiadiazole/phthalimide units (A2) as organic photosensitizers with D–A2–π–A1 configuration for solar cell applications, *J. Comput. Electronics,* 18 (2019) 375–395.

[31] Yanai, T., Tew, D.P., Handy, N.C., A new hybrid exchange-correlation functional using the Coulomb-attenuating method (CAM-B3LYP), *Chem. Phys. Lett.,* 393 (2004) 51–57.

[32] Zhao, Y., Truhlar, D.G., The M06 suite of density functionals for main group thermochemistry, thermochemical kinetics, noncovalent interactions, excited states, and transition elements: Two new functionals and systematic testing of four M06-class functionals and 12 other functionals, *Theor. Chem. Acc.,* 120 (2008) 215–241.

[33] Ernzerhof, M., Perdew, J.P., Generalized gradient approximation to the angle- and system-averaged exchange hole, *J. Chem. Phys.*, 109 (1998) 3313–3320.

[34] Vaissier, V., Barnes, P., Kirkpatrick, J., Nelson, J., Influence of polar medium on the reorganization energy of charge transfer between dyes in a dye-sensitized film, *Phys. Chem. Chem. Phys.,* 15 (2013) 4804-4814.

[35] Mendizabal, F., Mera-Adasme, R., Xu, W., Sundholm, D., Electronic and optical properties of metalloporphyrins of zinc on TiO_2 cluster in dye-sensitized solar cells (DSSC). A quantum chemistry study, *The Royal Society of Chemistry,* 7 (2017) 42677-42684.

[36] Yang, Z., Liu, Y., Liu, C., Lin, C., Shao, C., TDDFT screening auxiliary withdrawing group and design the novel D–A–π–A organic dyes based on indoline dye for highly efficient dye-sensitized solar cells, Spectrochim. *Acta A Mol. Biomol. Spectrosc.,* 167 (2016) 127–133.

[37] Hilal, R., Aziz, S.G., Osman, O.I., Bredas, J.L., Time-dependent—density functional theory characterization of organic dyes for dye-sensitized solar cells, *Mol. Simul.,* 43 (2017) 1523–1531.

[38] Arunkumar, A., Shanavas, S., Acevedo, R., Anbarasan, P.M., Acceptor tuning effect on TPA-based organic, efficient sensitizers for optoelectronic applications-quantum chemical investigation, *Structural Chemistry*, 31 (2020) 1029–1042.

[39] Jungsuttiwong, S., Tarsang, R., Sudyoadsuk, T., Promarak, V., Khongpracha, P., Namuangruk, S., Theoretical study on novel double donor-based dyes used in high efficient dye-sensitized solar cells: The application of TDDFT study to the electron injection process, *Org. Electron,* 14 (2013) 711–722.

[40] Fitri, A., Benjelloun, A.T., Benzakour, M., McHarfi, M., Hamidi, M., Bouachrine, M., Theoretical investigation of new thiazolothiazole-based D-π-A organic dyes for efficient dye-sensitized solar cell, *Spectrochim Acta. A Mol. Biomol. Spectrosc.,* 124 (2014) 646–654.

[41] Li, P., Cui, Y., Zhang, H., A systematic study of phenoxazine-based organic sensitizers for solar cells, *Dyes Pigm.*, 137 (2017) 12–23.

[42] Fu, J.J., Duan, Y.A., Zhang, J.Z., Guo, M.S., Liao, Y., Theoretical investigation of novel phenothiazine-based D–π–A conjugated organic dyes as dye-sensitizer in dye-sensitized solar cells, *Comput. Theor. Chem.*, 1045 (2014) 145–153.

[43] Mohamood, A., Triphenylamine based dyes for dye sensitized solar cells: A review, *Sol Energy* .123 (2016) 127-144.

[44] Lu, T.F., Li, W., Bai, F.Q., Anionic Ancillary Ligands in Cyclometalated Ru(II) Complex Sensitizers Improve Photovoltaic Efficiency of Dye-Sensitized Solar Cells: Insights from Theoretical Investigations. *J. Mater. Chem. A*, 5 (2017), 15567−15577.

[45] Xia, H.Q., Kong, C.P., Wang, J., Bai, F.Q., Zhang, H.X., Design of D–A–π–A organic dyes with different acceptor and auxiliary acceptor for highly efficient dye-sensitized solar cells: A computational study, *RSC. Adv.,* 4 (2014) 50338-50350.

[46] Souilah, M., Hachi, M., Fitri, A., Benjelloun, A.T., El Khattabi, S., Benzakour, M., Mcharf, M., Zgou, H., Coumarin based D–π–A dyes for efficient DSSCs: DFT and TD-DFT study of the π-spacers influence on photovoltaic properties, *Chemical Intermediates*, 47 (2020) 875–893.

[47] Tian, H., Yang, X., Cong, J., Chen, R., Teng, C., Liu, J., Hao, Y., Wang, L., Sun, L., Effect of different electron-donating groups on the performance of dye-sensitized solar cells, *Dyes Pigm.*, 84 (2010) 62–68.

[48] Li, W.Q., Wu, Y.Z., Zhang, Q., Tian, H., Zhu, W.H., D-A-π-A featured sensitizers bearing phthalimide and benzotriazole as the auxiliary acceptor: Effect on absorption and charge recombination dynamics in dye-sensitized solar cells, *ACS Appl. Mater. Interfaces,* 4 (2012) 1822−1830.

[49] Preat, J., Michaux, C., Jacquemin, D., Perpete, E.A., Enhanced efficiency of organic dye-sensitized solar cells: Triphenylamine derivatives, *J. Phys. Chem. C*, 113 (2009) 16821–16833.